International Journal of Pharmaceutics 383 (2010) 106–115

Contents lists available at ScienceDirect

International Journal of Pharmaceutics

journal homepage: www.elsevier.com/locate/ijpharm

Propranolol–magnesium aluminum silicate complex dispersions and particles: Characterization and factors influencing drug release

Sarasit Rojtanatanya, Thaned Pongjanyakul*

Faculty of Pharmaceutical Sciences, Khon Kaen University, 123 Mittraphab Road, Khon Kaen 40002, Thailand

ARTICLE INFO

Article history:
Received 16 July 2009
Received in revised form 25 August 2009
Accepted 6 September 2009
Available online 12 September 2009

Keywords:
Propranolol
Magnesium aluminum silicate
Complexes
Drug release
Molecular interaction

ABSTRACT

In this study, complexation of magnesium aluminum silicate (MAS) and propranolol HCl (PPN) in the form of dispersions and solid particles was investigated. PPN–MAS dispersions at different pHs were prepared and characterized. The physicochemical properties and *in vitro* drug release of the complexes were also examined. Incorporation of PPN into MAS dispersions at various pHs caused the formation of PPN–MAS flocculates with a different particle size, zeta potential and amount of PPN adsorbed. The PPN–MAS complexes prepared at various pHs were formed via cation exchange, hydrogen bonding and water bridging mechanisms, which were revealed by FTIR and solid-state ^{29}Si NMR spectroscopy. This led to the intercalation of PPN molecules into the silicate layers of MAS. *In vitro* drug release studies demonstrated that the kinetic release of PPN can be described using the particle diffusion controlled mechanism, suggesting that drug release was controlled by diffusion of the drug in aqueous channels in the particle matrix of the complexes. The PPN–MAS complexes provided a sustained-release of PPN after an initial burst release in acidic medium and pH 6.8 phosphate buffer when compared with the physical mixture and pure PPN powder. This was due to a slow diffusion of drug that was intercalated in the inside of the particle matrix. The preparation pH of the complexes did not influence the release of PPN; the important factors affecting drug release were particle size, percentage of drug loaded in the complexes and the type of release medium. This finding suggests that the PPN–MAS complexes obtained in this study are strong candidates for use as drug carriers in oral modified-release dosage forms.

1. Introduction

In pharmaceutics, complexation between drugs and biocompatible materials has been used for enhancement of drug solubility, drug stability, drug absorption and bioavailability (Martin, 1993). In recent years, clays and biocompatible inorganic materials have been applied to adsorb the drugs onto their structures because they have a large specific surface area, good adsorption ability and cation exchange capacity (Velde, 1992; Murray, 2000). It has been shown that the drug–clay complexes can retard and/or modulate the release of drugs (Trikeriotis and Ghanotakis, 2007; Park et al., 2008; Joshi et al., 2009). This finding led to the use of drug–clay complexes as drug carriers, and when the complexes are coated with a cationic polymer, a good drug release profile during a short period of time is observed (Park et al., 2008).

Magnesium aluminum silicate (MAS) is a mixture of natural smectite clays, specifically montmorillonite and saponite (Kibbe, 2000; Viseras et al., 2007). MAS has a layered structure that is constructed from tetrahedrally coordinated silica atoms fused into an edge-shared octahedral plane of either aluminum hydroxide or magnesium hydroxide (Alexandre and Dubois, 2000; Kibbe, 2000). The surface of the silicate layer contains numerous silanol groups (SiOH), which have the potential to form hydrogen bonds with other substances (Gupta et al., 2003). The separation of the layered structures occurs when they are hydrated in water, and the weakly positively charged edges and the negatively charged faces of MAS are then presented. The negatively charged faces on the silicate layers of MAS have strong electrostatic interactions with amine drugs (McGinity and Lach, 1977; Sánchez-Martin et al., 1981; Nunes et al., 2007; Pongjanyakul et al., 2009), thereby leading to the prolonged release of the drug. Due to the non-toxicity and non-irritation at the levels employed in pharmaceutical use (Kibbe, 2000), it is of interest to use MAS as a drug adsorbent to improve the physical characteristics and modulate drug release behavior. Recently, nicotine–MAS complexes were shown to enhance thermal stability of nicotine and provide a sustained-release of nicotine after an initial burst release (Pongjanyakul et al., 2009).

Propranolol hydrochloride (PPN) was the first β-adrenoceptor blocking drug to achieve wide therapeutic use in angina and hypertension (Dollery, 1991). It is a secondary amine compound, and its structure is shown in Fig. 1. Due to the short half life of PPN (3.9 h) (Dollery, 1991), PPN has been selected as a drug candidate

* Corresponding author. Tel.: +66 43 362092; fax: +66 43 202379.
E-mail address: thaned@kku.ac.th (T. Pongjanyakul).

0378-5173/$ – see front matter © 2009 Elsevier B.V. All rights reserved.
doi:10.1016/j.ijpharm.2009.09.016

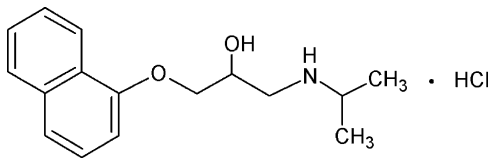

Fig. 1. Chemical structure of propranolol hydrochloride (PPN).

for developing sustained-release dosage forms (Gil et al., 2006; Sahoo et al., 2008; Paker-Leggs and Neau, 2009). However, many researchers in development of PPN sustained-release dosage forms were met with problems, such as the difficulty to control the release of the drug due to the high aqueous solubility of PPN. Thus, this problem may be solved by the complexation of PPN with MAS because the complexes obtained may retard the release of PPN. Sánchez-Martin et al. (1981) reported the interaction of PPN with montmorillonite; PPN can intercalate into the interlayer space of montmorillonite. However, there is no data available concerning other physicochemical properties or the *in vitro* release behavior of the PPN–montmorillonite complexes. Thus, it is necessary to study the physicochemical properties of PPN–MAS complexes in the form of dispersions and solid particles. The particle complexes obtained may be applicable as drug carriers for modulating PPN release.

In the present study, PPN–MAS dispersions at different pHs were prepared, and particle size, zeta potential of PPN–MAS flocculates, and drug adsorbed onto the MAS were investigated. Additionally, the physicochemical properties of the solid complexes such as thermal behavior, solid-state crystallinity, particle size and morphology were investigated. FTIR and solid-state ^{29}Si NMR spectroscopy were used to examine the molecular interaction between PPN and MAS within the complexes. The *in vitro* release behavior and release kinetics of PPN from the complexes using 0.1N HCl and pH 6.8 phosphate buffer were also examined.

2. Materials and methods

2.1. Materials

MAS (Veegum®HV) and PPN were purchased from the R.T. Vanderbilt Company Inc. (Norwalk, CT, USA) and Changzhou Yabang Pharmaceutical Co., Ltd. (Jiangsu, China), respectively. All other reagents used were of analytical grade and used as received.

2.2. Preparation of PPN–MAS dispersion

A 4% w/v MAS suspension was prepared using hot water and cooled to room temperature prior to use. Next, 25 ml of the 4% w/v MAS suspension was mixed with 25 ml of the 1% w/v PPN deionized water solution in an Erlenmeyer flask. The pH of all PPN–MAS dispersions were adjusted by adding a small amount of 1N HCl or 1N NaOH into the flask while swirling and using a pH meter (Ion Analyzer 250, Coring, USA) to determine when the final pH of the dispersions was 5, 7 or 9. Then the dispersions were incubated at 37 °C with shaking for 24 h to allow PPN adsorption into the MAS to equilibrate. The PPN–MAS dispersions prepared at various pHs were characterized as described below.

2.3. Characterization of PPN–MAS dispersions

2.3.1. Microscopic morphology studies

The morphology of the MAS particles and the PPN–MAS flocculates in the dispersions were investigated using an inverted microscope (Eclipse TS100, Nikon, Japan) and viewed using a digital camera (Coolpix 4500, Nikon, Japan).

2.3.2. Particle size determination

The particle size of the MAS particles and the PPN–MAS flocculates in the dispersions were measured using a laser diffraction particle size analyzer (Mastersizer2000 Model Hydro2000SM, Malvern Instrument Ltd., UK). The samples were dispersed in 70 ml of deionized water in a small volume sample dispersion unit and stirred at a rate of 50 Hz for 30 s before the measurement. The particle sizes (volume weighted mean diameter) were then recorded.

2.3.3. Zeta potential measurement

The zeta potential of the dispersions was measured by using a laser Doppler electrophoresis analyzer (Zetasizer Model ZEN 2600, Malvern Instrument Ltd., UK). The temperature of the samples was controlled at 25 °C. The dispersions were diluted using deionized water to obtain appropriate concentrations (count rates >20,000 counts per second) prior to measurement.

2.3.4. Determination of PPN adsorbed onto MAS

The clear supernatants of the dispersions were collected, filtered with a 0.45-μm cellulose acetate membrane, and then analyzed using UV–visible spectrophotometer (Shimadzu UV1201, Japan) at a wavelength of 289 nm. The amount of PPN adsorbed onto MAS was calculated as the difference between the amount of PPN added and the amount of PPN in the supernatant.

2.4. Preparation of PPN–MAS complexes

The PPN–MAS dispersions at various pHs were prepared using the method that was mentioned previously in Section 2.2. The PPN–MAS complexes were separated from the filtrates by filtration, washed 2 times with 20 ml of deionized water and dried overnight at 50 °C. For the second drug loading at pH 7, the PPN–MAS dispersions were prepared following the method in Section 2.2. The complexes collected from the first drug loading by filtration were redispersed in 25 ml of the 1% w/v PPN solution in an Erlenmeyer flask, and the mixture was incubated at 37 °C with shaking for 24 h. The PPN–MAS complexes of the double drug loading were separated, washed and dried following the method mentioned above. The dry PPN–MAS complexes were ground using a mortar and pestle and divided into 3 particle sizes using a sieving method: small size (passed through 125 μm sieve), medium size (125–180 μm sieve), and large size (180–250 μm sieve). The obtained complexes were kept in a desiccator prior to use. The small sized PPN–MAS complexes were used for investigation of PPN content and physicochemical properties. Additionally, the physical mixture between PPN and MAS was freshly prepared by gentle mixing in a small vial, in which the concentration of PPN was 14% (w/w) of the mixture.

2.5. Characterization of PPN–MAS complexes

2.5.1. Determination of PPN content

Fifty milligrams of the complexes were weighed and dispersed in 100 ml of 2N HCl for 24 h. Then the supernatant was collected and filtered, and the PPN content was assayed using a UV–visible spectrophotometer (Shimadzu UV1201, Japan) at a wavelength of 289 nm.

2.5.2. Particle size determination

The particle size of the complexes was measured using the same method mentioned in Section 2.3.2. The media used were 0.1N HCl and pH 6.8 phosphate buffer, and the volume weighted mean diameter of the particles was reported.

2.5.3. Scanning electron microscopy (SEM)

The particle shape and surface morphology of the MAS powder and the PPN–MAS complexes were observed using scanning elec-

Table 1
Characteristics of MAS and PPN–MAS dispersions.

Dispersion	Particle size[a] (μm)	Zeta potential[b] (mV)	PPN adsorption[a] (mg/1 g of MAS)	PPN content in flocculates (%w/w)
MAS dispersion	4.76 ± 0.12	−36.0 ± 1.1	–	–
PPN–MAS dispersion				
pH 5	141.8 ± 13.7	−10.2 ± 2.5	207.8 ± 2.4	17.21 ± 0.16
pH 7	134.1 ± 14.0	−12.4 ± 2.8	215.3 ± 1.5	17.71 ± 0.10
pH 9	125.1 ± 10.6	−15.0 ± 3.2	221.0 ± 0.2	18.10 ± 0.01

[a] Data are the mean ± SD of three determinations.
[b] Data are the mean ± SD of six determinations.

tron microscopy (SEM). Samples were mounted onto stubs, sputter coated with gold in a vacuum evaporator, and photographed using a scanning electron microscope (Jeol Model JSM-6400, Tokyo, Japan).

2.5.4. Powder X-ray diffractometry

Powder X-ray diffraction (PXRD) measurements of samples were performed on a powder X-ray diffractometer (Jeol Model JDX-3530, Tokyo, Japan). The measurement conditions were a Cu radiation generated at 40 kV and 40 mA as X-ray source, angular 3–25° (2θ), and step angle 0.02° (2θ) s^{-1}.

2.5.5. Fourier transform infrared (FTIR) spectroscopy

The FTIR spectra of samples were recorded with an FTIR spectrophotometer (Spectrum One, Perkin Elmer, Norwalk, CT) using the KBr disc method. Each sample was pulverized, gently triturated with KBr powder in a weight ratio of 1:100 and then pressed using a hydrostatic press at a pressure of 10 tons for 5 min. The disc was placed in the sample holder and scanned from 4000 to 450 cm^{-1} at a resolution of 4 cm^{-1}.

2.5.6. Nuclear magnetic resonance (NMR) spectroscopy

The ^{29}Si NMR spectra of the samples were measured using a solid-state ^{29}Si cross-polarization magic angle spinning (CP/MAS) NMR spectrometer (DPX-300, Bruker-BioSpin AG, Fällanden, Switzerland). The spectral parameters used were as follows: 1600 spins, a relaxation delay of 6 s, a spin rate of 5 kHz, and a spectral size of 4 K with a 2 K time domain size.

2.5.7. Differential scanning calorimetry (DSC)

DSC sample curves were recorded using a differential scanning calorimeter (DSC822, Mettler Toledo, Switzerland). Each sample (2–3 mg) was accurately weighed into a 40-μl aluminum pan and crimped without an aluminum cover. The measurements were performed in air over the range of 30–450 °C at a heating rate of 10 °C min^{-1}.

2.5.8. In vitro drug release studies

A USP dissolution apparatus 2 (paddle method, Hanson Research, USA) was used to characterize the release of PPN from the complexes. The amount of the PPN–MAS complexes used was equivalent to that containing 40 mg of PPN. The studies were performed in 500 ml of release medium at 37.0 ± 0.5 °C at a rotation speed of 50 rev/min. Samples (20 ml) were collected and replaced with fresh medium at various time intervals. The amount of PPN released was analyzed using a UV–visible spectrophotometer (Shimadzu UV1201, Japan) at a wavelength of 289 nm. The dissolution media used in this study were 0.1N HCl and pH 6.8 phosphate buffer.

The PPN release kinetic mechanism was investigated using a particle diffusion controlled model that has been previously proposed by Bhaskar et al. (1986). This model was applied to test the drug release from layered double hydroxides (Ni et al., 2008) and from MAS (Pongjanyakul et al., 2009), which can be expressed by the following equation (Bhaskar et al., 1986):

$$-\ln(1-F) = 1.59\left(\frac{6}{d_p}\right)^{1.3} D^{0.65} t^{0.65} \quad (1)$$

where F is the fractional release of drug from the complexes at given time (t), d_p is the mean particle size of the complexes, D is the apparent diffusion coefficient and t is time. This model can be investigated by simply testing for linearity between $-\ln(1-F)$ and $t^{0.65}$. The slope (drug release rate constant) of the straight line (estimated using linear regression analysis) was used to calculate the apparent diffusivity according to the following equation:

$$D = \frac{d_p^2}{36}\left(\frac{\text{slope}}{1.59}\right)^{1/0.65} \quad (2)$$

3. Results and discussion

3.1. Characteristics of PPN–MAS dispersions

The particle size, zeta potential, and PPN adsorption onto MAS in the composite dispersion prepared at different pHs are presented in Table 1. The mean particle size of MAS was found to be 4.76 μm with a negatively charged surface that had a zeta potential of −36.0 mV. The microscopic morphology of the MAS dispersion showed separated particles of MAS (Fig. 2a). Incorporation of PPN into the MAS dispersion caused a rapid sedimentation of MAS particles, indicative of the formation of PPN–MAS flocculates (Fig. 2b), which is due to the electrostatic interaction between negatively charged MAS and positively charged PPN. This led to an obvious decrease of the zeta potential of MAS (Table 1). Decreasing the preparation pH resulted in a reduction of both the zeta potential of the flocculates and percent of PPN adsorbed onto MAS; however, a larger particle size of the flocculates was observed when preparation pH was decreased. The zeta potential of the flocculates at pH 9 was higher than the zeta potential at pH 7 due to a lower degree of ionization of PPN at pH 9. The pK_a value of PPN is 9.5 (Dollery, 1991), and thus 75.8% of PPN was in the protonated form at pH 9. The protonated form of PPN increased to 99.7 and 99.9% at pH 7 and 5, respectively. The protonated form of PPN at pH 5 and 7 could potentially interact with the negatively charged MAS more readily than at pH 9, leading to increased adsorption of PPN onto the particle surface of MAS and a reduction of the electric barrier between the MAS particles, which was evident by a decrease in the zeta potential and the formation of a bridge between adjacent particles so as to link them together in a loosely arranged structure of flocculates (Martin, 1993). The lower the zeta potential, the larger the flocculate size was found. This result was in agreement with a previous study using nicotine and MAS (Suksri and Pongjanyakul, 2008). However, the PPN adsorbed onto MAS at pH 7 was lower than that at pH 9. It is probable that the larger flocculate size at neutral pH possessed lower surface area for PPN adsorption when compared with the smaller size of flocculates at pH 9. In comparison to pH 7, at pH 5 a reduction of the zeta poten-

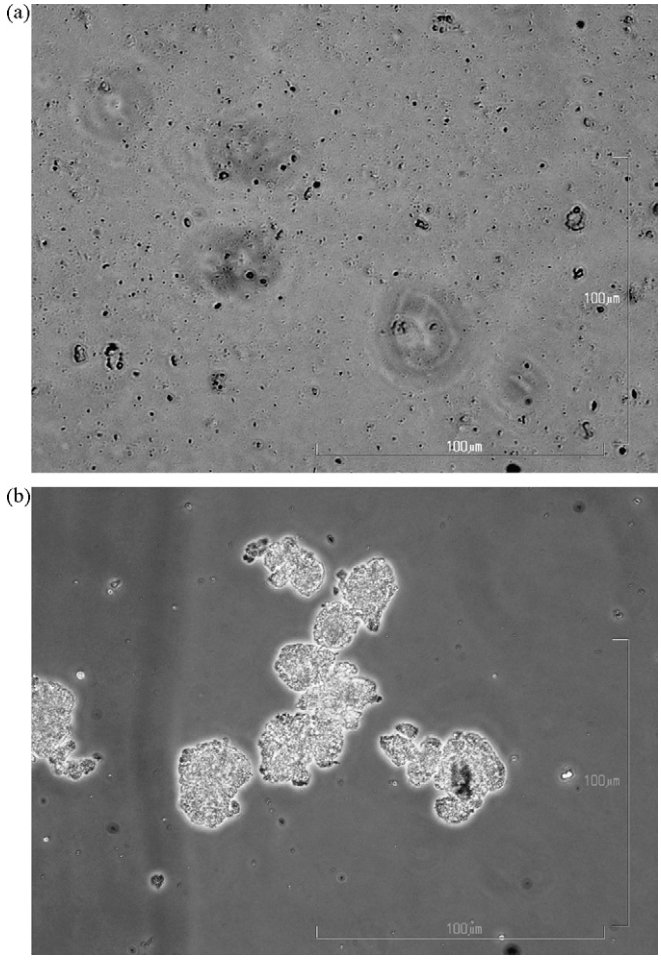

Fig. 2. Microphotographs of MAS particles in a MAS dispersion (a) and PPN–MAS flocculates in the composite dispersion prepared at pH 7 (b).

tial and increased flocculate size was observed, although both pHs displayed a similar degree of PPN ionization. This suggests that hydronium ions that increased at the lower pH could adsorb onto the MAS surface and partially neutralize the negative charge of MAS (Benna et al., 1999; Suksri and Pongjanyakul, 2008), thereby resulting in increased flocculate size and decreased PPN adsorbed onto the MAS. These results suggest that the pH of preparation influences the characteristics of the PPN–MAS flocculates in the composite dispersions, which may cause different physicochemical properties and drug release behavior of the obtained PPN–MAS complexes.

3.2. PPN content and particle size analysis

The PPN content of the PPN–MAS complexes prepared at pH 5, 7, and 9 by using a single drug loading was approximately 14% (w/w), which is listed in Table 2. It was observed that the PPN content of the dry complexes was significantly less than that of the complexes in the dispersions (Table 1). This was due to a loss of PPN from the surface of the complexes during the washing process with deionized water. Moreover, the PPN content of the complexes obtained from the double drug loading was significantly higher than that obtained from the single drug loading. This suggests that part of the adsorption site of MAS remained free after reaching adsorption equilibrium during the single drug loading, and the higher concentration of PPN in the second drug loading could drive the PPN adsorption onto the remaining site of MAS. Therefore, an increase in PPN content of the complexes was found when using a double loading of PPN.

The MAS particles were in a granular form and displayed many small flakes on the surface (Fig. 3a and b). The PPN–MAS complexes prepared at pH 7 (small size) had irregular shapes as shown in Fig. 3c and d. It was found that the PPN–MAS complexes had a different surface morphology when compared with that of MAS alone. The features of the small particles on the surface of the complexes were found to be caused by the aggregation of many small flocculates during the drying process.

The particle size of MAS granules dispersed in 0.1N HCl and pH 6.8 phosphate buffer was 50.4 ± 2.2 and $10.6 \pm 1.4\,\mu m$ ($n = 3$), respectively. The MAS particle size in both media was larger than in deionized water (Table 1). This suggests that cations in the medium influenced the dispersibility of MAS granules. On the other hand, the PPN–MAS complexes prepared at various pHs showed similar particle sizes generally in the range of medium size (Table 2). Moreover, neither media affected the particle size of the complexes (Table 2). These results suggest that the complexes could not disperse in 0.1N HCl and pH 6.8 phosphate buffer because a strong attraction force between the silicate layers of MAS formed upon interaction with PPN. The particle size obtained from this study was used to calculate the diffusion coefficient of PPN in the particle matrix of the complexes.

3.3. PXRD study

The MAS powder showed a distinct diffraction peak at 6.2° (2θ) (Fig. 4b), representing a 1.42-nm thickness of the silicate layer of MAS. The PPN–MAS complexes prepared at various pHs did not present the PXRD pattern of PPN alone (Fig. 4c–e), suggesting that PPN was in an amorphous form and molecularly dispersed onto the surface of the MAS silicate layer. However, the peak of the MAS powder at 6.2° (2θ) was shifted to 5.0° (2θ) (Fig. 4c–e) and gave stronger intensity when the PPN–MAS complexes occurred. This

Table 2
Particle size and PPN content of PPN–MAS complexes.

Condition of preparation	PPN content (%w/w)	Particle size (μm)	
		0.1N HCl	pH 6.8 phosphate buffer
Single loading (medium size)			
pH 5	14.13 ± 0.18	190.2 ± 1.0	196.6 ± 1.0
pH 7	14.51 ± 0.22	181.9 ± 0.4	189.8 ± 2.2
pH 9	14.42 ± 0.08	189.3 ± 0.4	190.4 ± 0.9
Double loading at pH 7	20.05 ± 0.60		
Small size		90.3 ± 0.7	89.3 ± 0.6
Medium size		203.9 ± 0.4	201.5 ± 0.8
Large size		259.4 ± 2.5	261.8 ± 1.1

Data are the mean ± SD of three determinations.

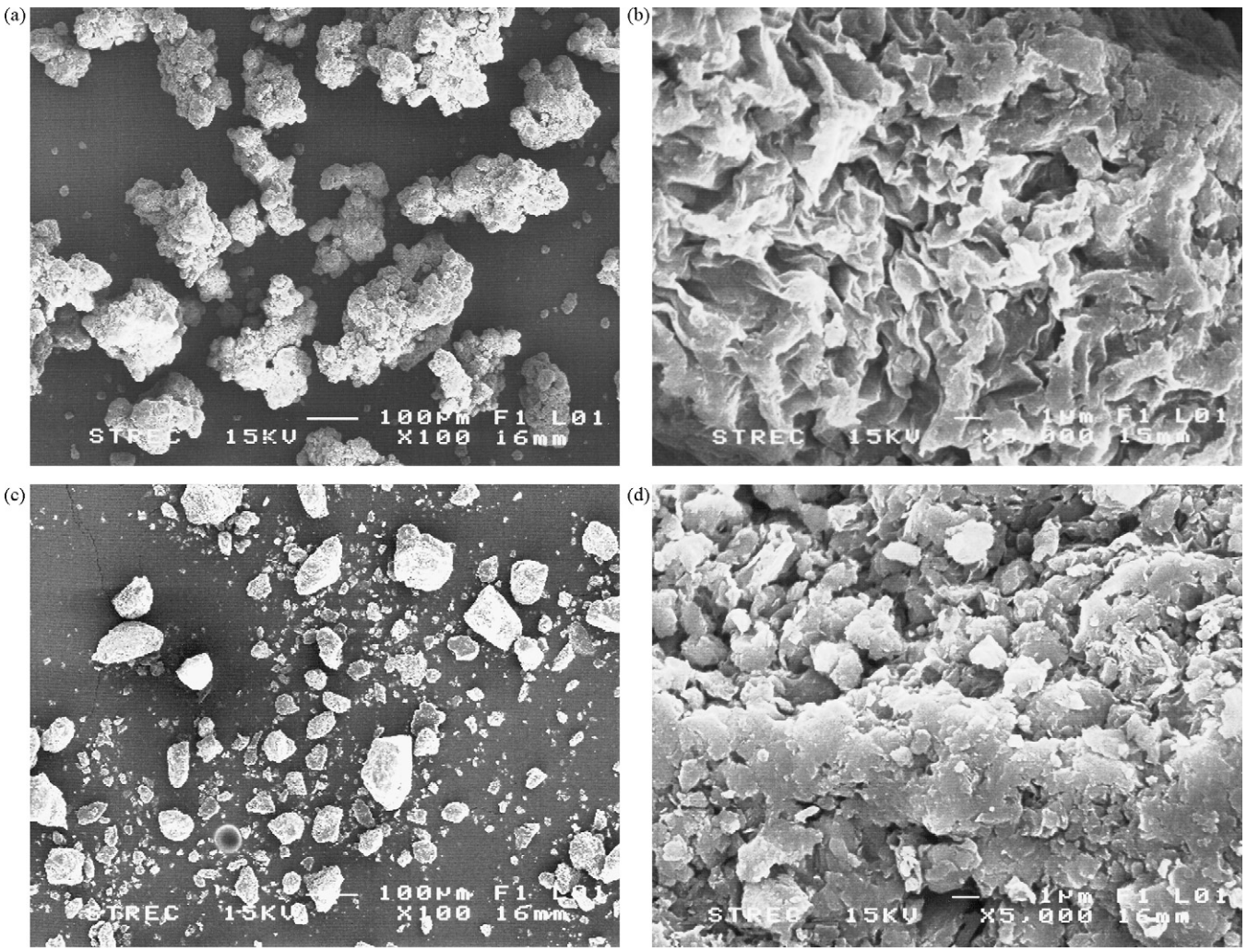

Fig. 3. Particle and surface morphology of MAS (a and b) and PPN–MAS complexes (c and d) prepared at pH 7 using a single loading (small size).

indicates that PPN can intercalate into the silicate layers of MAS because the MAS layer thickness was increased to approximately 1.77 nm. Moreover, a previous study showed that a stronger intensity of the basal spacing peak occurs when the drug molecule is intercalated into the silicate layers of MAS (Pongjanyakul et al., 2009). This may be due to an increased stacking of the intercalated silicate layers (Sinha Ray et al., 2003), which resulted from the interaction between MAS and PPN.

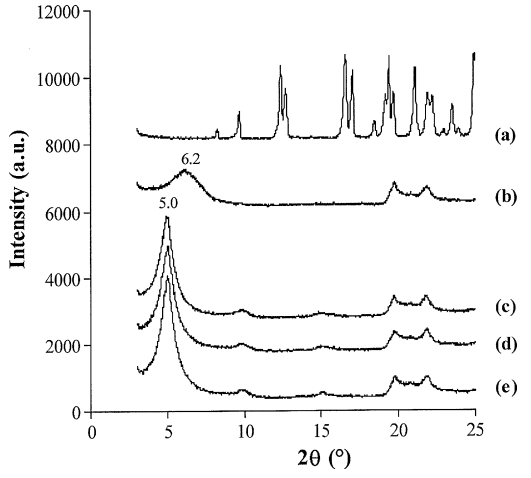

Fig. 4. PXRD patterns of PPN (a), MAS (b), and PPN–MAS complexes prepared at pH 5 (c), 7 (d), and 9 (e).

3.4. Interaction between PPN and MAS

The molecular interaction between PPN and MAS was elucidated by using FTIR spectroscopy. The FTIR spectra of PPN showed N–H and O–H stretching peaks at 3323 and 3283 cm^{-1} (Fig. 5a), respectively, which was an essential peak for detecting the interaction of PPN with MAS. The outstanding peaks of MAS were the O–H stretching peak of SiOH at 3632 cm^{-1}, the O–H stretching peak of water residues at 3447 cm^{-1}, the O–H bending peak of water crystallization at 1640 cm^{-1}, and the Si–O–Si stretching peak at 1016 cm^{-1} (Fig. 5b). The physical mixture between PPN and MAS presented a shift of the N–H and O–H stretching peaks of PPN to 3332 and 3279 cm^{-1} (Fig. 5c), respectively. It is possible that the amine and hydroxyl groups of PPN may have potentially interacted with MAS during gentle mixing. However, no obvious changes in the peaks of MAS were observed. The PPN–MAS complexes prepared at various pHs showed a remarkable change of the MAS peaks (Fig. 5d–f). The O–H stretching peak at 3447 cm^{-1} and the O–H bending peak at 1640 cm^{-1} strongly shifted to lower wavenumbers at 3429–3435 cm^{-1} and 1630 cm^{-1}, respectively. This suggests that in the complexes, water bound with PPN and/or MAS via hydrogen bonding. These data indicate that the interaction between PPN

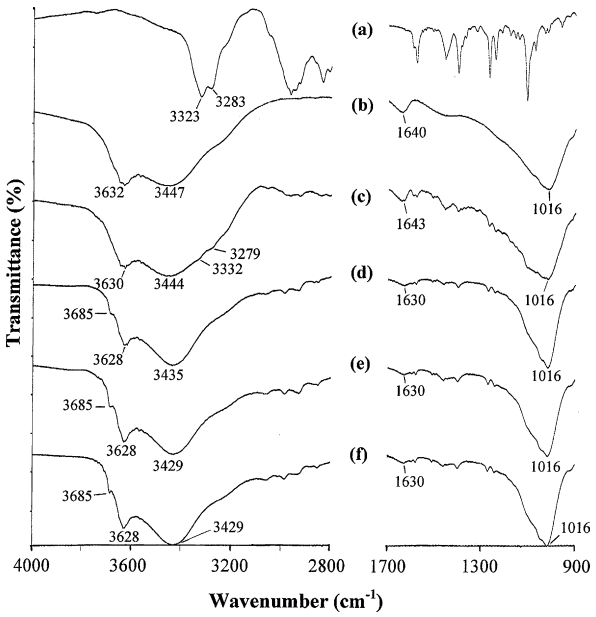

Fig. 5. FTIR spectra of PPN (a), MAS (b), physical mixture (c) and PPN–MAS complexes prepared at pH 5 (d), 7 (e), and 9 (f).

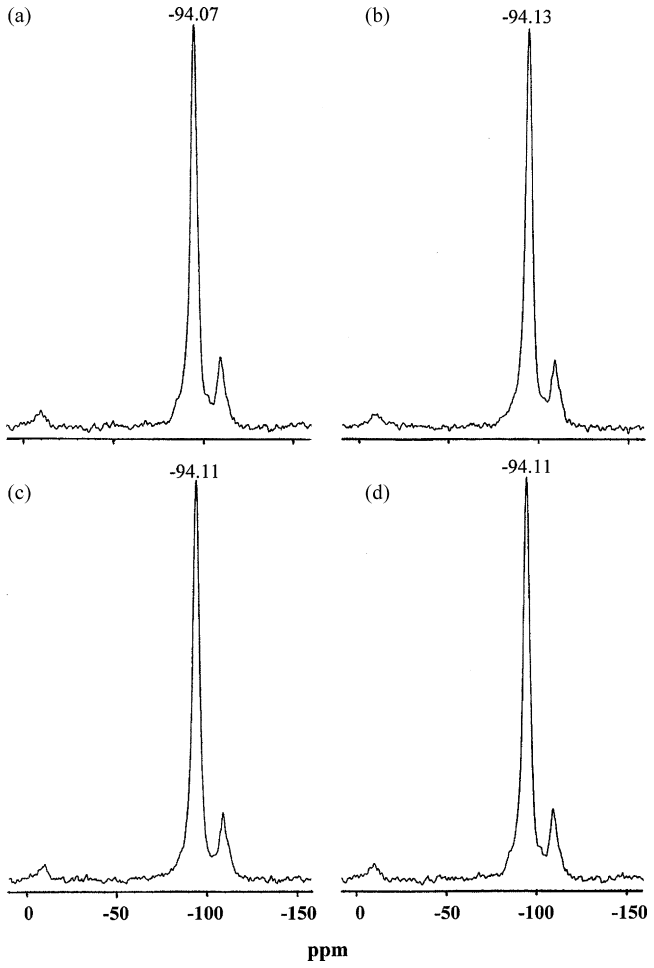

Fig. 6. Solid-state ^{29}Si NMR spectra of MAS (a) and PPN–MAS complexes prepared at pH 5 (b), 7 (c), and 9 (d).

and MAS occurred via the water bridging mechanism (Aguzzi et al., 2007; Pongjanyakul et al., 2009). The O–H stretching peak of SiOH at 3632 cm^{-1} was sharper and shifted to a lower wavenumber (3628 cm^{-1}), and the N–H and O–H stretching peaks of PPN were not observed, which can be attributed to the hydrogen bonding formation of silanol groups (SiOH) of MAS with the amine and hydroxyl groups of PPN. Additionally, the occurrence of the new peak at 3685 cm^{-1} (Fig. 5d–f) after the formation of the PPN–MAS complexes indicates free OH groups on the inner surface of the silicate layer of MAS (Hoch and Bandara, 2005). The stronger vibration of free hydroxyl groups on the inner surface of the silicate layers was able to occur when the basal spacing of the MAS silicate layers increased due to the intercalation of the PPN molecules, which was demonstrated by PXRD. This result was similar with a previous report that observed this phenomenon in nicotine–MAS complexes (Pongjanyakul et al., 2009).

The electrostatic interaction between PPN and MAS was expected. The solid-state ^{29}Si NMR spectra of the MAS and the PPN–MAS complexes are illustrated in Fig. 6. The ^{29}Si NMR spectra give evidence of electronic changes in the tetrahedral sheet of montmorillonite. The ^{29}Si chemical shift of −94.07 ppm of MAS to −94.13, −94.11, and −94.11 ppm of the complexes at pH 5, 7, and 9, respectively, was found. Additionally, the Si–O–Si stretching peak (1016 cm^{-1}) of the complexes (Fig. 5d–f) was narrower than that of MAS alone. The slightly negative change in the chemical shift and the narrower Si–O–Si stretching peak indicates a decrease in the charge of the MAS layer (Gates et al., 2000).

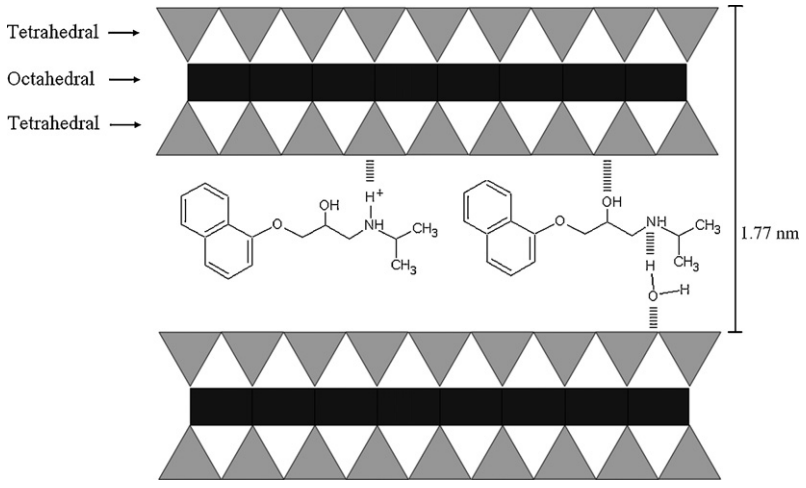

Fig. 7. Possible structure arrangement of PPN–MAS complexes.

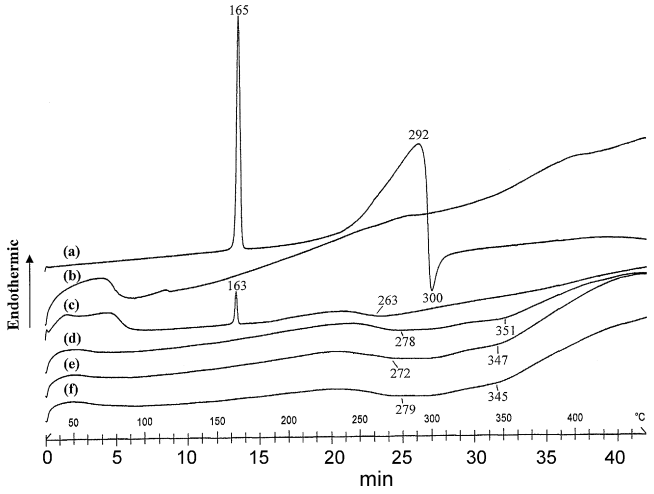

Fig. 8. DSC thermograms of PPN (a), MAS (b), physical mixture (c), and PPN–MAS complexes prepared at pH 5 (d), pH 7 (e) and pH 9 (f).

According to the results obtained from the FTIR and ^{29}Si NMR spectroscopy as well as PXRD, it can be suggested that complexation between PPN and MAS formed via electrostatic interaction by cation exchange, hydrogen bonding, and the water bridging mechanism, which can occur at various pHs. This led to the possible structure arrangement of the PPN–MAS complexes as illustrated in Fig. 7.

3.5. Thermal behavior

The DSC thermogram of PPN showed a sharp endothermic peak at 165 °C (Fig. 8a), indicating the melting point of PPN. A broad endothermic peak at 292 °C followed by an exothermic peak at 300 °C represented the decomposition of PPN. MAS presented a broad endothermic peak at 70 °C, which was attributable to the dehydration of free water residues (Fig. 8b). The PPN–MAS physical mixture had an endothermic peak at 163 °C, indicative of a melting peak of PPN, and a broad exothermic peak was observed at 263 °C, suggesting the degradation of PPN in the physical mixture (Fig. 8c). For the PPN–MAS complexes, the absence of a melting peak of PPN suggests a molecular dispersion and amorphous form of PPN in the complexes, which confirmed the results of PXRD. The complexes prepared at various pHs presented two broad exothermic peaks at around 272–279 °C and 345–351 °C (Fig. 8d–f). This is likely due to both the decomposition of PPN adsorbed onto the particle surface of the complexes and the PPN that was intercalated in the silicate layers of MAS.

3.6. In vitro release of PPN–MAS complexes

The effect of preparation pH and particle size of the PPN–MAS complexes on PPN release profiles using 0.1N HCl and pH 6.8 phosphate buffer are shown in Figs. 9 and 10, respectively. As shown in Fig. 11, the relationship between $-\ln(1-F)$ and $t^{0.65}$ of the PPN released from the complexes showed a good linearity. This relationship presented two stages of PPN release after the burst release at 2 min, and the slope (release rate constant) obtained was used to compute the diffusion coefficient (D value) shown in Table 3. The PPN released from a freshly prepared physical mixture of PPN with MAS and PPN powder was also investigated. In both media, the PPN powder was completely dissolved within 2 min of the test. The physical mixture showed very fast release with 65–74% drug released at 2 min in both media (Table 3), and then the amount of PPN released gradually decreased (Fig. 9), suggesting that the

Table 3
PPN release characteristics of PPN–MAS complexes.

PPN–MAS	0.1N HCl					pH 6.8 phosphate buffer					
	Drug released at 2 min (%)	Slope × 10^2 (min$^{-0.65}$)		D value × 10^{10} (cm^2 s^{-1})		Drug released at 2 min (%)	Slope × 10^2 (min$^{-0.65}$)		D value × 10^{10} (cm^2 s^{-1})	
		Stage 1	Stage 2	Stage 1	Stage 2		Stage 1	Stage 2	Stage 1	Stage 2
Physical mixture	74.1 ± 3.7	–	–	–	–	65.6 ± 5.9	–	–	–	–
Complexes (single loading, medium size)										
pH 5	11.9 ± 0.3	2.00 ± 0.07 (R^2 = 0.946)	1.17 ± 0.06 (R^2 = 0.996)	2.00 ± 0.11	0.88 ± 0.07	8.08 ± 0.55	2.18 ± 0.06 (R^2 = 0.966)	0.44 ± 0.01 (R^2 = 0.986)	2.44 ± 0.10	0.21 ± 0.01
pH 7	15.1 ± 0.4	2.06 ± 0.26 (R^2 = 0.965)	1.28 ± 0.09 (R^2 = 0.993)	1.92 ± 0.37	0.92 ± 0.09	6.25 ± 0.06	1.79 ± 0.22 (R^2 = 0.865)	0.63 ± 0.07 (R^2 = 0.977)	1.68 ± 0.33	0.34 ± 0.06
pH 9	13.0 ± 0.8	1.73 ± 0.50 (R^2 = 0.973)	1.10 ± 0.04 (R^2 = 0.997)	1.62 ± 0.74	0.79 ± 0.04	9.20 ± 0.25	1.71 ± 0.06 (R^2 = 0.968)	0.81 ± 0.06 (R^2 = 0.991)	1.58 ± 0.08	0.50 ± 0.06
Complexes (pH 7, double loading)										
Small size	71.8 ± 2.3	–	1.63 ± 0.08 (R^2 = 0.983)	–	0.33 ± 0.02	51.6 ± 1.1	–	1.64 ± 0.07 (R^2 = 0.986)	–	0.33 ± 0.02
Medium size	37.9 ± 1.5	5.66 ± 0.65 (R^2 = 0.980)	3.31 ± 0.70 (R^2 = 0.987)	11.4 ± 2.0	5.05 ± 1.67	37.7 ± 1.6	8.82 ± 1.36 (R^2 = 0.936)	1.43 ± 0.29 (R^2 = 0.989)	22.0 ± 5.1	1.36 ± 0.42
Large size	27.1 ± 0.4	8.56 ± 1.22 (R^2 = 0.997)	4.15 ± 0.52 (R^2 = 0.994)	35.0 ± 7.8	11.5 ± 2.2	31.7 ± 1.0	8.27 ± 0.67 (R^2 = 0.939)	1.41 ± 0.28 (R^2 = 0.993)	33.7 ± 4.2	2.24 ± 0.66

Data are the mean ± SD of three determinations.

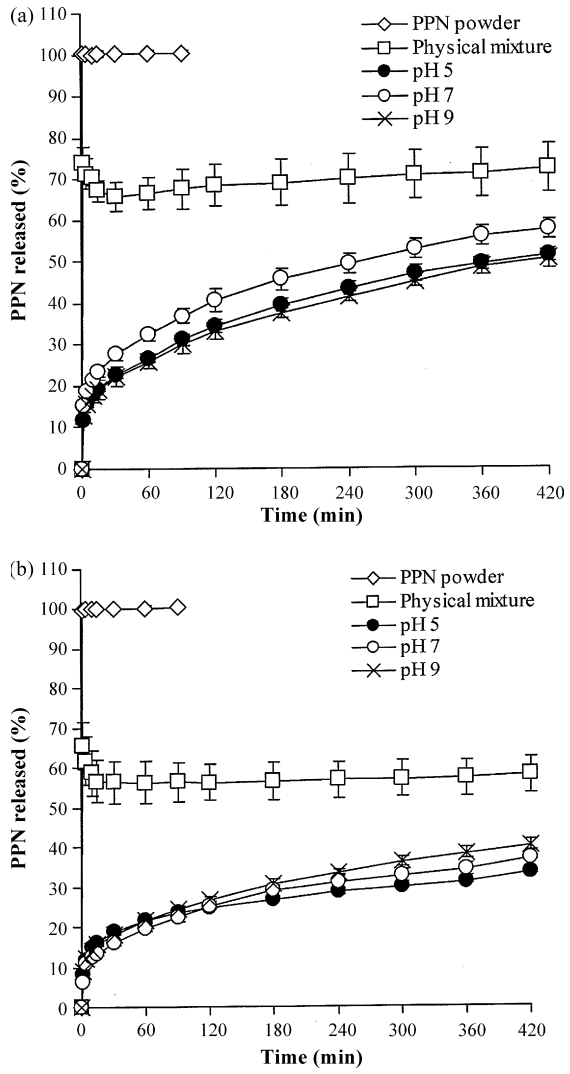

Fig. 9. PPN release profiles of PPN powder, physical mixture, and PPN–MAS complexes prepared at various pHs using a single loading in 0.1N HCl (a) or pH 6.8 phosphate buffer (b). Each point is the mean ± SD, $n = 3$.

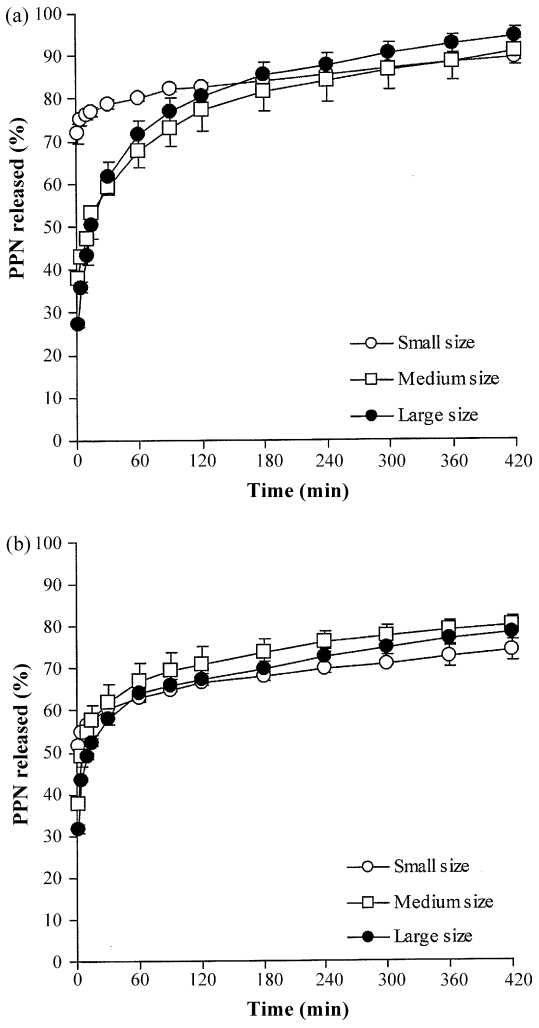

Fig. 10. Effect of particle size on PPN released from PPN–MAS complexes prepared at pH 7 using a double loading in 0.1N HCl (a) or pH 6.8 phosphate buffer (b). Each point is the mean ± SD, $n = 3$.

PPN that was released could be readsorbed by the MAS dispersed in the release medium. The PPN–MAS complexes showed a slow release profile, and the preparation pH did not influence the release of PPN from the complexes (Fig. 9). This was observed from the drug released at 2 min, and release rate constants are shown in Table 3. The release rate constant in stage 2 was lower than that in stage 1 because of the reduction of the drug concentration gradient in the complex particle. No difference was observed in the release rate constant of stage 1 between the two media, whereas a higher release rate constant of stage 2 in acidic medium was obtained when compared with using pH 6.8 phosphate buffer. This difference was also found in the D values. Apart from the effect of preparation pH, particle size also had a strong influence on the drug release. It was observed that the drug released at 2 min significantly increased with decreasing particle size of the complexes (Table 3). In contrast, increasing release rate constants were found for the larger particle sizes, particularly in the acidic medium. Additionally, the D values in both stages increased with increasing particle size of the complexes.

This study shows that release of PPN from the complexes is controlled by a particle matrix that acts as a diffusion barrier for drug release. This was due to a good fit of the PPN release data using the particle diffusion controlled model. When the particles of the

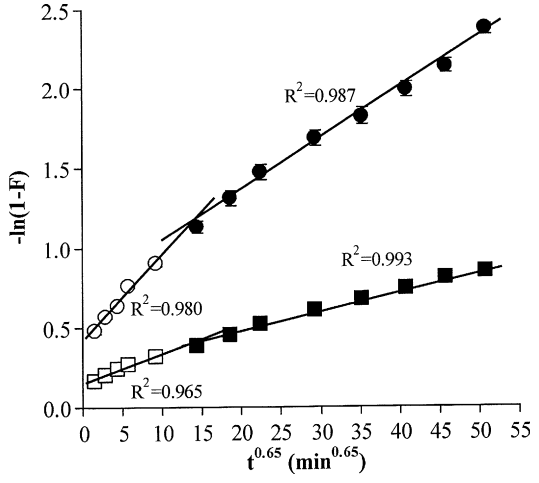

Fig. 11. Relationship between $-\ln(1 - F)$ and $t^{0.65}$ of PPN–MAS complexes prepared at pH 7 using a single (□) or double (○) loading in 0.1N HCl. Open and closed symbols represented drug release data at stages 1 and 2, respectively, and the solid line is the linear regression line of each drug release stage. Each point is the mean ± SD, $n = 3$.

complexes are exposed to the dissolution medium, the simultaneous penetration of the surrounding medium and cation exchange process occurred, thereby leading to a burst release (drug released at 2 min) of the PPN adsorbed onto the particle surface of the complexes. Then the cations diffuse into the particles to exchange with the PPN adsorbed and intercalated in the silicate layers of MAS, which leads to the leaching out of PPN through interstitial aqueous channels. After which, the diffusion of PPN molecules through numerous aqueous channels within the particle matrix occurs. These processes can describe the first stage of drug release. However, in this study the PPN–MAS complexes also demonstrated a second stage of drug release. It is probable that this stage represents the drug released and diffused from the silicate layer space of the MAS, which could be called a nanostructure matrix, on the inside of the particles of the complexes. This resulted in a lower release rate constant and *D* value.

The preparation pH of the PPN–MAS complexes did not obviously affect the PPN release. These results were similar to a previous report using complexes of nicotine and MAS (Pongjanyakul et al., 2009). This is likely due to the similar mechanism of complex formation at the different pHs, which was hydrogen bonding, water bridging, and the cation exchange process, which led to the similar PPN release profiles in acidic medium and pH 6.8 phosphate buffer. However, the use of 0.1N HCl showed increase PPN release than pH 6.8 phosphate buffer, even though the cation concentration of 0.1N HCl (100 mequiv./l) was not different from that of pH 6.8 phosphate buffer (99.7 mequiv./l). Therefore, the factors affecting the release of PPN were both the type of cation and pH of the medium. Generally, hydrogen ions (28 pm) have smaller ionic radii than sodium ions (161 pm) (Heyrovska, 2009). This leads to faster diffusion into the particles of the complexes. Moreover, MAS has high affinity for hydrogen ions in the acidic medium because it had a lower zeta potential in this condition when compared with the neutral pH medium (Suksri and Pongjanyakul, 2008). Taken together, these reasons explain why faster release of PPN in the acidic medium was observed. Furthermore, it was observed that the PPN released at 7 h in the acidic medium was higher than that in pH 6.8 phosphate buffer (Figs. 9 and 10), indicating that the smaller size of hydrogen ions could diffuse deep into the inside of the particles of the complexes for the cation exchange process.

The particle size of the complexes is one of the important factors influencing drug release. It was found that the larger the particle size of the complexes, the lower the initial burst release (drug released at 2 min). This was due to decreased specific surface area of the large size particles. Higher release rate constants and *D* values were obtained from the large size particles. This can potentially be explained by the higher remaining of PPN content in the larger size complexes compared to the smaller size complexes after the initial burst release, leading to a higher concentration gradient of PPN in the large size complexes. This brought about faster drug release, which increased the calculated *D* values. Furthermore, increasing drug loading from 14% (w/w) to 20% (w/w) of the complexes prepared at pH 7 (medium size) caused an increase in drug released at 2 min and release rate constant (Table 3). The higher PPN content in the complexes provided a reduction of the relative amount of diffusional barrier material in the complexes. Moreover, the higher drug loading also created a larger drug concentration gradient in the complexes when exposed to the release medium. The higher the concentration gradient, the faster the mass transfer, resulting in the increased drug release rate constant and *D* values obtained in this study.

The PPN–MAS complexes provided a slow release of PPN after the burst release in acidic medium within 7 h of the test, during which equilibrium of drug release was not reached. Moreover, the PPN release at 7 h was more than 89% for 0.1N HCl and 74% for pH 6.8 phosphate buffer. Park et al. (2008) reported that donepezil–montmorillonite complexes have a 12% drug release at 180 min in simulated human gastric medium supplemented with a cationic polymer to enhance drug release. It is possible that because PPN has a lower molecular weight than donepezil, this led to an increased rate of diffusion of PPN in aqueous channels of the particle matrix. The low amount of drug released using the larger donepezil molecule could be due to a very slow diffusion of drug that was adsorbed and intercalated in the inside of the particles of the complexes. Additionally, the PPN–MAS complexes showed a faster drug release rate than the nicotine–MAS complexes in the same range of particle size, which used the same preparation method (Pongjanyakul et al., 2009). Smaller nicotine molecules contain two protonated amino groups that possibly have very high affinity for MAS. This led to the slower rate of release of nicotine when compared with PPN. This suggests that the drug release behavior of drug–clay complexes is also dependent upon the properties of the intercalated drug such as its molecular weight and chemical structure.

4. Conclusions

The study presented herein demonstrated that the interaction of PPN and MAS caused a flocculation in the composite dispersion at various pHs, resulting in a change of particle size and zeta potential of MAS and a different amount of PPN adsorbed onto MAS. The complexation between PPN and MAS was created via cation exchange, hydrogen bonding and water bridging mechanisms, which led to the intercalation of PPN molecules into the MAS silicate layers. The PPN–MAS complexes provided a sustained-release of PPN after an initial burst release, and the PPN release kinetics were described using the particle diffusion controlled model. The preparation pH did not influence the release of PPN; the important factors affecting drug release were particle size, percent of drug loading of the complexes and the type of release medium. This study suggests that these PPN–MAS complexes have a strong potential to be employed as drug carriers in oral modified-release dosage forms. Further work to evaluate the drug release of polymer matrix tablets containing PPN–MAS complexes is currently ongoing.

Acknowledgments

The authors would like to thank the Thailand Research Fund (Bangkok, Thailand) for research funding (Grant no. RSA5280013). We are very pleased to acknowledge the Center for Research and Development of Herbal Health Products and the Faculty of Pharmaceutical Sciences, Khon Kaen University (Khon Kaen, Thailand), for technical support.

References

Aguzzi, C., Cerezo, P., Viseras, C., Caramella, C., 2007. Use of clays as drug delivery systems: possibilities and limitations. Appl. Clay Sci. 36, 22–36.

Alexandre, M., Dubois, P., 2000. Polymer-layered silicate nanocomposites: preparation, properties and uses of a new class of materials. Mater. Sci. Eng. 28, 1–63.

Benna, M., Kbir-Ariguib, N., Magnin, A., Bergaya, F., 1999. Effect of pH on rheological properties of purified sodium bentonite suspensions. J. Colloid Interface Sci. 218, 442–455.

Bhaskar, R., Murthy, R.S.R., Miglani, B.D., Viswanathan, K., 1986. Novel method to evaluate diffusion controlled release of drug from resinate. Int. J. Pharm. 28, 59–66.

Dollery, S.C., 1991. Therapeutic Drugs. Churchill Livingstone, Edinburgh, pp. P272–P278.

Gates, W.P., Komadel, P., Madejová, J., Bujdák, J., Stucki, J.W., Kirkpatrick, R.J., 2000. Electronic and structural properties of reduced-charge montmorillonite. Appl. Clay Sci. 16, 257–271.

Gil, E.C., Colarte, A.I., Bataille, B., Pedraz, J.L., Rodríguez, F., Heinämäki, J., 2006. Development and optimization of a novel sustained-release dextran tablet formulation for propranolol hydrochloride. Int. J. Pharm. 317, 32–39.

Gupta, M.K., Vanwert, A., Bogner, R.H., 2003. Formation of physical stable amorphous drugs by milling with Neusilin. J. Pharm. Sci. 92, 536–551.
Heyrovska, R., 2009. Golden sections of inter-atomic distances as exact ionic radii of atoms. Nature Precedings (http://hdl.handle.net/10101/npre.2009.2929.1).
Hoch, M., Bandara, A., 2005. Determination of the adsorption process of tributyltin (TBT) and monobutyltin (MBT) onto kaolinite surface using Fourier transform infrared (FTIR) spectroscopy. Colloids Surf. A 253, 117–124.
Joshi, G.V., Kevadiya, B.D., Patel, H.A., Bajaj, H.C., Jasra, R.V., 2009. Montmorillonite as a drug delivery system: intercalation and in vitro release of timolol maleate. Int. J. Pharm. 374, 53–57.
Kibbe, H.A., 2000. Handbook of Pharmaceutical Excipients, 3rd ed. American Pharmaceutical Association, Washington, pp. 295–298.
Martin, A., 1993. Physical Pharmacy, 4th edition. Lea&Febiger, Philadelphia, pp. 251–283.
McGinity, J.W., Lach, J.L., 1977. Sustained-release application of montmorillonite interaction with amphetamine sulfate. J. Pharm. Sci. 66, 63–66.
Murray, H.H., 2000. Traditional and new applications for kaolin, smectite, and palygorskite: a general overview. Appl. Clay Sci. 17, 207–221.
Ni, Z., Xing, F., Wang, P., Cao, G., 2008. Synthesis, characterization and release of curcumin-intercalated Mg–Al-layered double hydroxides. Appl. Clay Sci. 40, 72–80.
Nunes, C.D., Vaz, P.D., Fernandes, A.C., Ferreira, P., Romão, C.C., Calhorda, M.J., 2007. Loading and delivery of sertraline using inorganic micro and mesoporous materials. Eur. J. Pharm. Biopharm. 66, 357–365.
Paker-Leggs, S., Neau, S.H., 2009. Pellet characteristics and drug release when the form of propranolol is fixed as moles or mass in formulations for extruded and spheronized Carbopol-containing pellets. Int. J. Pharm. 369, 96–104.
Park, J.K., Choy, Y.B., Oh, J., Kim, J.Y., Hwang, S., Choy, J., 2008. Controlled release of donepezil intercalated in smectite clays. Int. J. Pharm. 359, 198–204.
Pongjanyakul, T., Khunawattanakul, W., Puttipipatkhachorn, S., 2009. Physicochemical characterizations and release studies of nicotine–magnesium aluminum silicate complexes. Appl. Clay Sci. 44, 242–250.
Sahoo, J., Murthy, P.N., Biswal, S., Sahoo, S.K., Mahapatra, A.K., 2008. Comparative study of propranolol hydrochloride release from matrix tablets with Kollidon®SR or hydroxy propyl methyl cellulose. AAPS Pharm. Sci. Technol. 9, 577–582.
Sánchez-Martin, M.J., Sánchez-Camazano, M., Vicente-Hernández, M.T., Dominguez-Gil, A., 1981. Interaction of propranolol hydrochloride with montmorillonite. J. Pharm. Pharmacol. 33, 408–410.
Sinha Ray, S., Yamada, K., Okamoto, M., Ogami, A., Ueda, K., 2003. New polylactide/layered silicate nanocomposites: 3. High performance biodegradable materials. Chem. Mater. 15, 1456–1465.
Suksri, H., Pongjanyakul, T., 2008. Interaction of nicotine with magnesium aluminum silicate at different pHs: characterization of flocculate size, zeta potential and nicotine adsorption behavior. Colloids Surf. B. 65, 54–60.
Trikeriotis, M., Ghanotakis, D.F., 2007. Intercalation of hydrophilic and hydrophobic antibiotics in layered double hydroxides. Int. J. Pharm. 332, 176–184.
Velde, B., 1992. Introduction to Clay Minerals. Chapman & Hall, London, pp. 12–36.
Viseras, C., Aguzzi, C., Cerezo, P., Lopez-Galindo, A., 2007. Uses of clay minerals in semisolid health care and therapeutic products. Appl. Clay Sci. 36, 37–50.